Decadal Changes in CCSM3.5 ENSO Dynamics

Samantha Stevenson[1], Baylor Fox-Kemper[1] and Markus Jochum[2]
[1]ATOC/CIRES, University of Colorado at Boulder, Boulder, CO
[2]National Center for Atmospheric Research (NCAR), Boulder, CO

Abstract
Recent updates to the atmospheric convection scheme in CCSM3.5 have yielded a more accurate representation of ENSO than any previous incarnation of CCSM. However, within a long model run the behavior of ENSO shifts on decadal timescales - even when the mean state remains the same. This study applies the multitaper method/singular value decomposition (MTM-SVD) to diagnose distinct dynamical modes within ENSO. The frequencies of interest are shown to change during periods of high/low ENSO activity, as well as the appearance of those modes. Both delayed oscillator-like and recharge/discharge-like dynamics are seen, indicating that it may be an interaction between these modes which is responsible for generating differences in overall ENSO variability.

Same mean state, different dynamics

	Years	σ_{NINO3} (C^2)	Δz_{th} (m)	Mean z_{th} (m)	u (m/s)	σ_u (m^2/s^2)
P_LO	350-399	0.534	91.58	95.82	-14.64	0.517
P_HI	600-649	1.041	93.36	97.51	-14.86	0.528

The model run used in this study is a 700-year integration under pre-industrial conditions. During two 50-year intervals having nearly identical mean states, **NINO3 variance differs by a factor of 2!**

Identifying modes: MTM-SVD

The multitaper method/singular value decomposition (MTM-SVD) analysis used here is a decomposition in both the spatial and spectral dimensions. A Fourier transform is applied to the time series at each model grid point, then spectra are separated into orthogonal components using Slepian sequences. Finally, the matrix of (complex) spectra is subjected to a singular value decomposition to identify the spatial pattern associated with that mode of variability. The resulting set of orthogonal modes retains phase information, allowing the sequence of events in all fields (here, SST, thermocline depth and zonal wind stress) to be determined for each mode.

Model years 350-399: "P_LO" **Model years 600-650: "P_HI"**

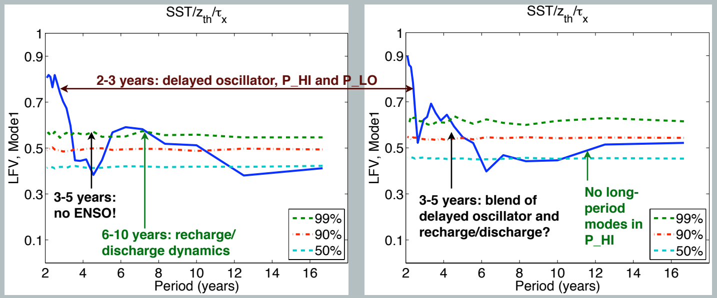

Local Fractional Variance (LFV) for the dominant mode of oscillation in P_LO and P_HI, with bootstrap confidence intervals overlaid. ENSO-like patterns are seen where modes are significant at > 90%.

Delayed Oscillator: P_HI, 2.1 years

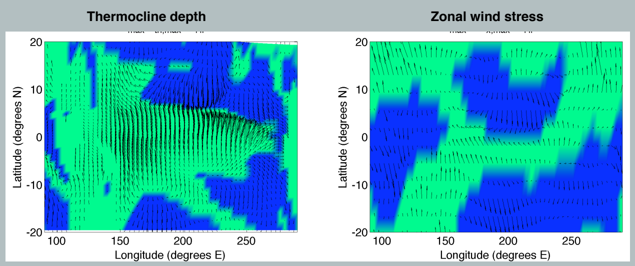

Recharge/Discharge: P_LO, 6.25 years

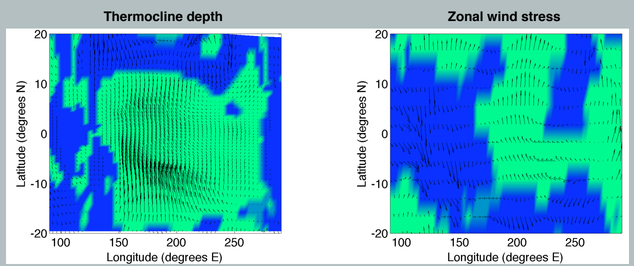

Arrow plots for P_HI mode 1 at 2.1 years (left) and P_LO mode 1 at 6.25 years (right). Amplitude of oscillation is reflected in the length of the arrows; the angle represents the phase lag relative to NINO3. Shaded green areas lead SST; shaded blue areas lag SST.

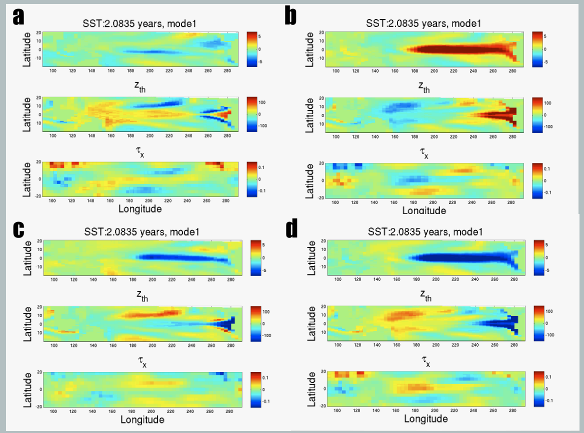

At 2.1 years in P_HI, wave dynamics are visible. Kelvin waves travel eastward across the equator (panel a), to set up the El Niño phase of the oscillation (panel b). When the signal reaches the eastern boundary, an off-equatorial Rossby wave signal is created, propagating westward (panel c) across the basin.

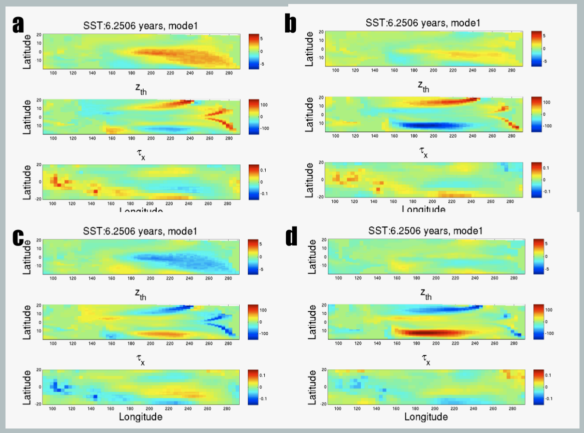

At 6.25 years in P_LO, dynamics are visibly different. The equatorial Kelvin wave signal has vanished, replaced by an alternating north/south thermocline signal. This signal is accompanied by a large wind stress curl and associated Sverdrup transport, driving heat in and out of the basin.

Waves vs. wind stress curl

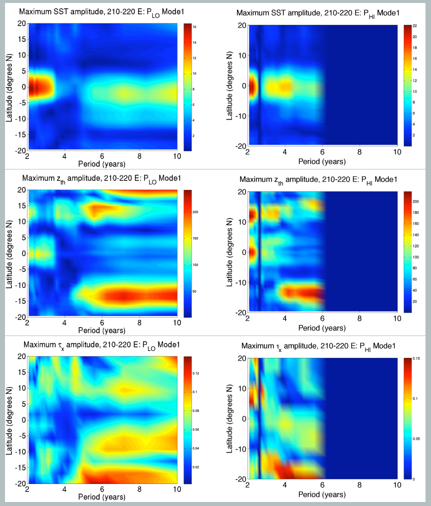

At left are shown the amplitude of oscillations in SST, thermocline depth and zonal wind stress as a function of oscillation period and latitude, averaged over 210-220 E (central Pacific). Here distinct patterns are seen in P_HI and P_LO. Below ~3.5 years, oscillations in the Northern Hemisphere dominate; at longer periods the opposite seems to be true in both P_HI and P_LO. Additionally, in P_LO from 6-10 years a strong thermocline depth signal is seen at ~15 S, where the gradient in zonal wind stress is largest. This is characteristic of recharge/discharge dynamics.

Conclusions

The vastly improved ENSO in CCSM3.5 shows dramatic changes on decadal timescales, even under constant forcing conditions. Even during periods having the same mean state, total NINO3 variance may change by a factor of 2.

We have used MTM-SVD analysis to identify distinct dynamical modes driving ENSO within the model, and find that modes having the appearance of both "delayed oscillator" and "recharge/discharge" dynamics are present. However, the relative importance of these dynamics changes with time within the run; in particular, recharge/discharge dynamics are much more important during "P_LO", when model ENSO is 2x weaker than during "P_HI". We hypothesize that this is due to an overall discharge of heat from the basin during P_LO, making all ENSO modes less efficient.

This represents a first cut at examining model ENSO dynamics under pre-industrial conditions; additional work is necessary to catalog the full range of dynamical variability.